A Coordinated DP Control Methodology for the MOB

K. Hedrick, A. Girard, and B. Kaku*

ABSTRACT

There are many proposed concepts for a future Mobile Offshore Base (MOB). All concepts attempt to form a runway suitable for C-17 size transport aircraft by positioning large controllable semi-submersibles to form an interconnected runway. Some concepts involve rigid connections between the vessels, which are established once they are close enough together. Other concepts rely on continuously acting steerable thrusters to keep the vessels properly aligned. It is the latter approach that we will investigate here. This paper develops a fully nonlinear DP controller design methodology that can be implemented in either a robust form or an adaptive parameter estimation form. Next, the modifications required to coordinate the control of three vessels will be developed. In general it is desirable to have the vessels pointing into the wind while maintaining the desired relative surge, sway, and yaw accuracies necessary to permit aircraft landings on the interconnected runway. Several control hierarchies will be simulated and evaluated with respect to both the resulting control performance and energy consumption. All simulations will be carried out using the "Shift" simulation software developed at PATH. The first concept evaluated will be a "follow-the-leader" model where the first vessel in the three vessel string, designated as the "leader," will be controlled to track a desired inertial heading, longitude, and latitude. The second and third vessels will track the relative positions of the first and second vessels, respectively. Although this is a small string, it may still suffer from "string instability" problems (i.e. spacing errors may amplify along the string). The second concept to be evaluated will be a follow-the-leader scheme with the middle vessel chosen as the leader. String stability should not be a problem here since both following vessels directly track the leader. The final concept to be evaluated is a "leaderless" scheme where each vessel is controlled to track both an inertial reference as well as its position with respect to adjacent vessels. Keywords: Nonlinear control design, dynamic positioning (DP), leaderless control, Shift simulation software, multiple sliding surface (MSS) control, dynamic surface control (DSC).

*khedrick@euler.berkeley.edu

I. NONLINEAR CONTROL OF ONE VESSEL

The nonlinear equations which describe the low-frequency horizontal motion of a surface vessel may be written as (Fossen, 1994, Newman, 1977):

$$(M_{RB} + M_A)\dot{\nu} + C_{RB}(\nu)\nu + C_A(\nu_r)\nu_r = F_{env} + F_T \qquad (1)$$

In this equation, M_{RB} and M_A are the body mass and added mass matrices, C_{RB} and C_A are the body coriolis/centripetal and added coriolis/centripetal matrices, and $\nu = [u \quad v \quad r]^T$ is a vector of body-fixed velocity components in the surge, sway, and yaw directions. $\nu_r = [u_r \quad v_r \quad r]^T$ is a vector of body-fixed relative velocity components, where the relative velocity is the velocity of the vessel relative to the water. F_{env} contains the body-fixed components of wind forces, viscous current forces, and second-order wave forces. F_T contains the body-fixed thruster force components: surge force, sway force, and yaw moment. The body-fixed velocity components are related to the earth-fixed velocity components by:

$$\dot{\eta} = J(\eta)\nu \qquad (2)$$

where

$$\dot{\eta} = \begin{bmatrix} \dot{x} \\ \dot{y} \\ \dot{\psi} \end{bmatrix} \text{ and } J(\eta) = \begin{bmatrix} \cos(\psi) & -\sin(\psi) & 0 \\ \sin(\psi) & \cos(\psi) & 0 \\ 0 & 0 & 1 \end{bmatrix}$$

For the purposes of controller design, we will simplify the problem by assuming zero current velocity and neglecting the environmental disturbance forces. Equation 1 can then be written as:

$$M\dot{\nu} + C(\nu)\nu = F_T \qquad (3)$$

where $M = M_{RB} + M_A$ and $C(\nu)\nu = C_{RB}(\nu)\nu + C_A(\nu)\nu$. Equations 2 and 3 describe the system dynamics which will be studied in this paper. The control problem is to choose F_T such that the vessel reaches desired inertial coordinates, $\eta_d = [x_d \quad y_d \quad \psi_d]^T$. We will utilize the "Multiple Sliding Surface" (MSS) (Won and

Hedrick, 1996) and "Dynamic Surface Control" (DSC) (Swaroop, et. al. , 1997) methods as well as the "Slotine and Li" algorithm (Slotine and Li, 1991), which was adapted to the control of underwater vehicles by Fossen (1994).

The MSS controller involves two "sliding surfaces". The first surface defines the desired vessel position and orientation. The second surface defines a desired velocity, which, if maintained, will drive the vessel to its desired position. Thruster forces are chosen such that the second surface approaches zero.

The first surface is defined as:

$$s_1 = \eta - \eta_d \tag{4}$$

differentiating s_1 yields,

$$\dot{s_1} = J(\eta)\nu - \dot{\eta_d}$$

At this point a desired velocity, or "synthetic control", ν_d is defined by,

$$J(\eta)\nu_d = \dot{\eta_d} - \Lambda_1 s_1 \tag{5}$$

where Λ_1 is a positive definite matrix. With this definition, if $\nu \equiv \nu_d$, then,

$$\dot{s_1} = -\Lambda_1 s_1 \tag{6}$$

and $s_1 \to 0$ with a convergence rate determined by the choice of Λ_1. Because of the definition of s_1, this will also guarantee that $\eta \to \eta_d$.

The second sliding surface could be defined as $s_2 = \nu - \nu_d$, but computing $\dot{s_2}$ would require differentiation of Equation 5, which could lead to a very complex control law. A method described by Swaroop et. al. (1996) called "Dynamic Surface Control" (DSC) eliminates the need for model differentiation. First, we pass ν_d through a bank of first order filters:

$$T\dot{z} + z = \nu_d \tag{7}$$

where T is a diagonal matrix whose elements, T_{ii}, are the filter time constants. These are chosen to be as small as possible, consistent with numerical conditioning problems. z now serves as an estimate of ν_d, with a derivative which is easily computed as

$$\dot{z} = T^{-1}(\nu_d - z) \tag{8}$$

Using z in place of ν_d, we now define the second sliding surface as:

$$s_2 = \nu - z \tag{9}$$

At this point, a Lyapunov approach (Slotine and Li, 1991) can be drawn upon. Define a Lyapunov function candidate by:

$$V = \frac{1}{2} s_2^T M s_2$$

Differentiating V and using Equations 3 and 9 yields,

$$\begin{aligned} \dot{V} &= s_2^T \left[M\dot{\nu} - M\dot{z} \right] \\ &= s_2^T \left[F_T - C(\nu)\nu - M\dot{z} \right] \end{aligned} \tag{10}$$

If F_T is selected as:

$$F_T = C(\nu)\nu + M\dot{z} - K_D s_2 \tag{11}$$

then

$$\dot{V} = -s_2^T K_D s_2$$

which guarantees that $s_2 \to 0$. This, in turn, implies that $\nu \to \nu_d$, $s_1 \to 0$, and $\eta \to \eta_d$. Using Equation 8, the control law can be written in terms of z:

$$F_T = C(\nu)\nu + MT^{-1}(\nu_d - z) - K_D s_2 \tag{12}$$

When the model parameters are not perfectly known, the controller must be implemented using estimated parameters. In this case, Equation 11 becomes:

$$F_T = \hat{C}(\nu)\nu + \hat{M}\dot{z} - K_D s_2 \tag{13}$$

where $\hat{C}$ and $\hat{M}$ are the estimated values of C and M. With gain matrix K_D chosen large enough, this control can keep s_2 arbitrarily close to zero even in the presence of large modeling errors. Therefore, this is a robust controller.

For a number of reasons, achieving robustness through the use of high gains is often undesirable. An alternative approach for dealing with parameter uncertainty is to use an adaptation algorithm, such as the one outlined in Slotine and Li (1991). If the unknown parameters are constants which appear linearly in the system equations, then Equation 13 can be written in the form:

$$F_T = Y(\nu, \dot{z})\hat{a} - K_D s_2 \tag{14}$$

where $\hat{a}$ is a $p \times 1$ vector of estimated model parameters and Y is an exactly known $3 \times p$ matrix.

Define a candidate Lyapunov function by:

$$V = \frac{1}{2} s_2^T M s_2 + \frac{1}{2} \tilde{a}^T \Gamma^{-1} \tilde{a}$$

where $\tilde{a} = \hat{a}(t) - a$, a is the vector of unknown constants, and Γ is a symmetric positive definite matrix. By differentiating and substituting, $\dot{V}$ is found to be:

$$\dot{V} = -s_2^T K_D s_2 + \left(s_2^T Y + \dot{\hat{a}}^T \Gamma^{-1} \right) \tilde{a}$$

If the parameter adaptation law is defined as:

$$\dot{\hat{a}} = -\Gamma Y^T s_2 \tag{15}$$

then,

$$\dot{V} = -s_2^T K_D s_2 \tag{16}$$

This guarantees that $s_2 \to 0$, even in the presence of model error. The complete adaptive control law to be implemented consists of Equations 4, 5, 7, 9 , 14, and 15.

II. CONTROL OF MULTIPLE VESSELS

The previous section outlined a nonlinear robust and a nonlinear adaptive control strategy for a single MOB vessel. This section discusses the control of multiple coordinated vessels to form a runway straight enough for aircraft operations.

There are a great number of different possible strategies for coordinating multiple vessels. The goal of every strategy is to position the vessels in a straight line with tight relative spacing constraints. The line should be oriented in inertial space so that the formed runway points into the wind. An important consideration in the control of multiple vessels is the concept of "string stability," (Swaroop, et. al. , 1996) which states that small perturbations between vessels should not be amplified to successive vessels.

In this paper, three different strategies are investigated for coordinated multiple vessel control. It will be assumed that the MOB formation consists of three vessels. For all three control strategies, MSS will be used. The MSS approach is very convenient for the decentralized control of dynamically interacting systems since the design of the higher levels can be decoupled from the lower levels. As in the single vessel problem, the surfaces define desired vessel positions and velocities.

A. Follow-the-Leader Control

The first two strategies to be designed and analyzed employ "follow-the-leader" structures.

A.1. First Vessel As Leader

In this design, the first of the three vessels is chosen to be the leader.

First Vessel Denoting the desired inertial position of the first vessel by $\eta_d^1 \triangleq \left[x_d^1, y_d^1, \psi_d^1\right]^T$, where the superscript indicates the vessel number, the first surface for the first vessel becomes, $s_1^1 = \eta^1 - \eta_d^1$. From this point, the procedure outlined in the previous section is followed:

$$\nu_d^1 = J^{-1}(\eta^1)\left[\dot{\eta}_d^1 - \Lambda_1 s_1^1\right]$$

$$T\dot{z}^1 + z^1 = \nu_d^1$$

$$s_2^1 = \nu^1 - z^1$$

The required actuator forces for the vessel are computed using Equation 12.

Second Vessel The second vessel will simply attempt to maintain a desired spacing relative to the first, with no information about the desired inertial coordinates. The first surface is defined as:

$$s_1^2 = \eta^2 - \eta^1 - \eta_d^{21}$$

The first two terms are the actual relative spacing while the last term is the desired relative spacing. The resulting design becomes:

$$\nu_d^2 = J^{-1}(\eta^2)\left[\dot{\eta}^1 + \dot{\eta}_d^{21} - \Lambda_r s_1^2\right]$$

$$T\dot{z}^2 + z^2 = \nu_d^2$$

$$s_2^2 = \nu^2 - z^2$$

Again, the required actuator forces are computed using Eqn. 12.

Since maintaining the relative spacing between vessels is a higher priority than maintaining the inertial coordinates of the runway, the diagonal elements of Λ_r would be chosen to be larger than the diagonal elements of Λ_1.

Third Vessel The third vessel attempts to track the second vessel in the same fashion as the second vessel tracks the first, with controller variables defined by:

$$s_1^3 = \eta^3 - \eta^2 - \eta_d^{32}$$

$$\nu_d^3 = J^{-1}(\eta^3)\left[\dot{\eta}^2 + \dot{\eta}_d^{32} - \Lambda_r s_1^3\right]$$

$$T\dot{z}^3 + z^3 = \nu_d^3$$

$$s_2^3 = \nu^3 - z^3$$

A.2. Second Vessel As Leader

The previous design may have a problem with "string stability" since the third vessel has no knowledge of the desired inertial coordinates, and is not tracking an "inertial" vessel. Small angular motions by the leader, for instance, can result in significant sway motions for the third vessel. For a three vessel string, this problem can be reduced by defining the second vessel as the leader. The resulting first surface definitions are given below:

1^{st} vessel : $s_1^1 = \eta^1 - \eta^2 - \eta_d^{12}$
2^{nd} vessel : $s_1^2 = \eta^2 - \eta_d^2$
3^{rd} vessel : $s_1^3 = \eta^3 - \eta^2 - \eta_d^{32}$

B. Leaderless Control

An alternative strategy that has several attractive features is a "leaderless" control design. In this design, each vessel is given desired inertial coordinates that fall on a line with the correct heading and relative spacing. In addition, the surfaces are designed to maintain the desired relative spacing during transient conditions. The primary surfaces are defined as weighted combinations of absolute and relative errors:

$$s_1^1 = \eta^1 - \eta_d^1 + \Lambda_r(\eta^1 - \eta^2 - \eta_d^{12})$$

$$s_1^2 = \eta^2 - \eta_d^2 + \Lambda_r(\eta^2 - \eta^1 - \eta_d^{21}) + \Lambda_r(\eta^2 - \eta^3 - \eta_d^{23})$$

$$s_1^3 = \eta^3 - \eta_d^3 + \Lambda_r(\eta^3 - \eta^2 - \eta_d^{32})$$

By adjusting the diagonal elements of Λ_r, the importance of absolute vs relative errors can be changed, with higher values corresponding to tighter relative position accuracies. The synthetic body-fixed velocities, ν_d^i are chosen by solving:

$$\dot{s_1^i} = -\Lambda_1 s_1^i$$

which results in:

$$\nu_d^1 = J^{-1}(\eta^1)(I + \Lambda_r)^{-1}\left[\dot{\eta}_d^1 + \Lambda_r(\dot{\eta}^2 + \dot{\eta}_d^{12}) - \Lambda_1 s_1^1\right]$$

$$\nu_d^2 = J^{-1}(\eta^2)(I + 2\Lambda_r)^{-1}\left[\dot{\eta}_d^2 + \Lambda_r(\dot{\eta}^1 + \dot{\eta}_d^{21} + \dot{\eta}^3 + \dot{\eta}_d^{23}) - \Lambda_1 s_1^2\right]$$

$$\nu_d^3 = J^{-1}(\eta^3)(I + \Lambda_r)^{-1}\left[\dot{\eta}_d^3 + \Lambda_r(\dot{\eta}^2 + \dot{\eta}_d^{32}) - \Lambda_1 s_1^3\right]$$

Some of the attractive features of this approach are: 1) there is guaranteed string stability since each vessel has an inertial reference, and 2) the identical control structure can be used for both decoupled and coupled maneuvers. If it is desired to decouple the vessels and send them to arbitrary locations, then $\Lambda_r \equiv 0$ and η_d^i is defined for each separate vessel.

III. SHIFT SIMULATION

Shift is a programming language for describing dynamic networks of hybrid automata (Shift Team, 1996-1997). Such systems consist of components which can be created, interconnected, and destroyed as the system evolves. Components exhibit hybrid behavior, which consists of continuous-time phases separated by discrete-event transitions. Components may evolve independently, or they may interact through their inputs, outputs, and exported events. The interaction network itself may evolve. The Shift model offers a high level of abstraction for describing complex applications, and has successfully been applied to automated highway systems, air traffic control systems, robotics, shopfloors, coordinated submarines, and other systems whose operation cannot be captured easily by conventional models. A Shift model of the MOB platform dynamics and control systems has been developed.

For this paper, the robust algorithm for three vessels under leaderless and follow-the-leader control schemes is tested in Shift. For both control approaches, $T = diag\{5,5,5\}$, $\Lambda_1 = diag\{0.01, 0.01, 0.01\}$, $\Lambda_r = diag\{1,1,1\}$, and $K_d = diag\{0.1M(1,1), 0.1M(2,2), 0.1M(3,3)\}$ where M is the mass matrix. The M and C matrices are taken to be, $M = diag(6.353\times10^7\ slugs, 4.8006\times10^7\ slugs, 1.4286\times10^{13}\ lbf-ft^2)$ and:

$$C = \begin{bmatrix} 0 & 0 & c_{13} \\ 0 & 0 & c_{23} \\ c_{31} & c_{32} & 0 \end{bmatrix}$$

where, $m_c = 4.434 \times 10^7\ slugs$, $c_{13} = -m_c v - 3.66 \times 10^7 v$, $c_{23} = m_c u + 1.199 \times 10^7 u$, $c_{31} = m_c v + 3.66 \times 10^7 v$, $c_{32} = -m_c u - 1.199 \times 10^7 u$. Note that M is symmetric and C is skew-symmetric. The values are based on preliminary designs done by Bechtel National.

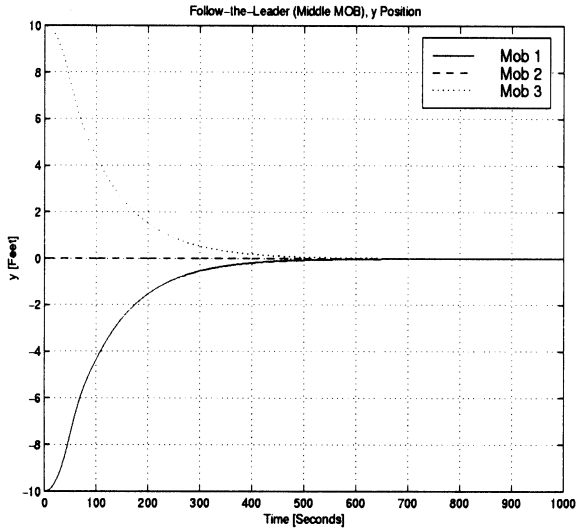

Figure 1. y Position, Follow-the-Leader (Middle MOB) Control

The thruster dynamics are modeled as a first order filter with a 3 second time constant. Force and moment saturation limits are also imposed on the thrusters.

Finally, all simulations were run in Matlab in order to verify the Shift results.

A. Stationkeeping

The first scenario simulates stationkeeping along the x-axis. The three vessels are initially perturbed from the desired overall horizontal orientation. Figures 1 - 6 highlight the behavior of the individual vessels as they return to the desired stationkeeping position under leaderless and follow-the-leader control schemes. The vessels start at $\eta_0^1 = [-2000\ ft, -10\ ft, 0\ rad]$, $\eta_0^2 = [0\ ft, 0\ ft, 0.05\ rad]$, and $\eta_0^3 = [2000\ ft, 10\ ft, 0.1\ rad]$. The desired final positions, aligned on the x-axis, are, $\eta_d^1 = [-2000\ ft, 0\ ft, 0\ rad]$, $\eta_d^2 = [0\ ft, 0\ ft, 0\ rad]$, and $\eta_d^3 = [2000\ ft, 0\ ft, 0\ rad]$.

Follow-the-Leader Control Follow-the-leader control was simulated for the cases of the first vessel and the middle vessel as leader. Only the results for the middle vessel as leader are presented here because this scheme displays better performance in aligning the overall MOB. Figures 1 and 2 show the y and angular positions of the vessels. One can see that the y-positions converge to their desired values with no overshoot or steady state error. Figure 2 shows typical follow-the-leader behavior as MOB vessel 1 overshoots its desired angular position in order to follow MOB vessel 2 (middle vessel). Figure 3 shows the relative angular positions of the vessels with respect to one another.

Leaderless Control Figures 4 and 5 show the y and angular positions of the MOBs with leaderless control. The convergence of y-position is faster under leaderless control when compared to follow-the-leader control, while convergence of absolute angular position is roughly the same. However, the relative angular position, shown in Figures 3 and 6, reaches zero significantly faster under leaderless control than with follow-the-leader (350 vs. 750 seconds). This indicates that leaderless control does a better job of aligning the MOB vessels in a straight line.

B. Aligning Into the Wind

In this maneuver, the vessels move from a horizontal alignment (the stationkeeping position) to a straight line arrangement, rotated -10^0 with respect to the x-axis, using leaderless control.

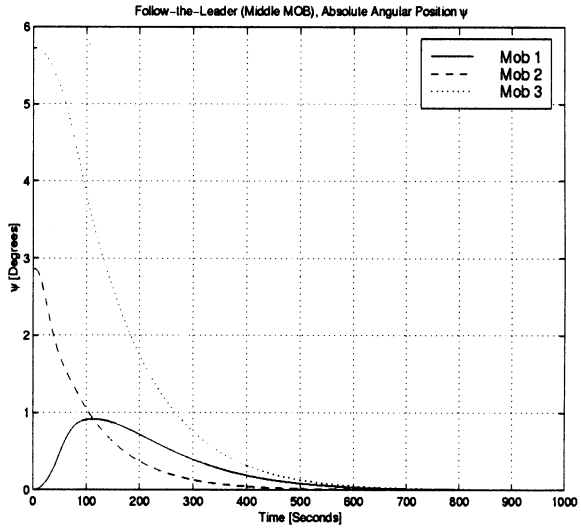

Figure 2. Absolute Angular Positions ψ, Follow-the-Leader (Middle MOB) Control

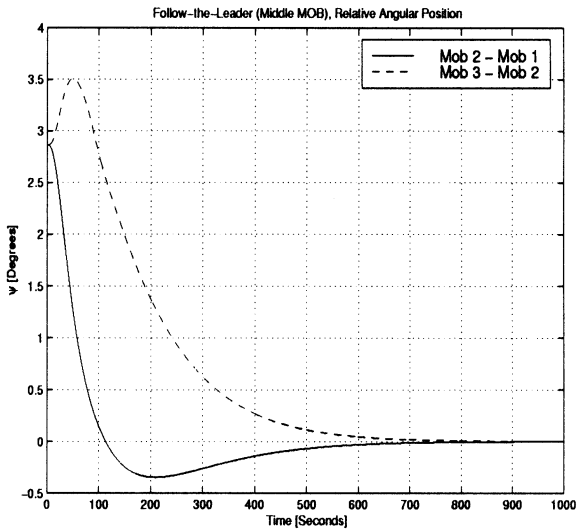

Figure 3. Relative Angular Positions, Follow-the-Leader (Middle MOB) Control

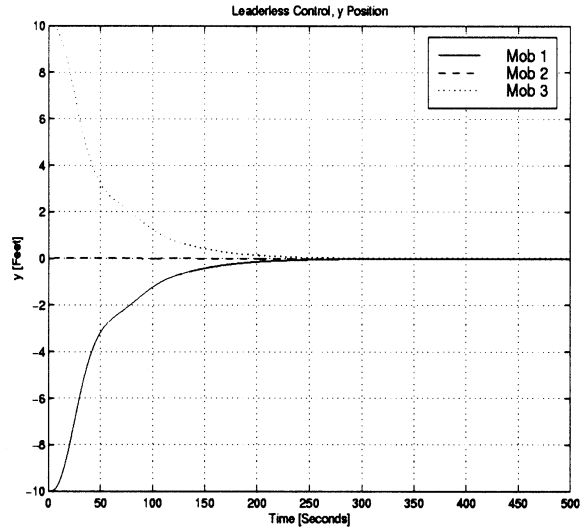

Figure 4. y Position, Leaderless Control

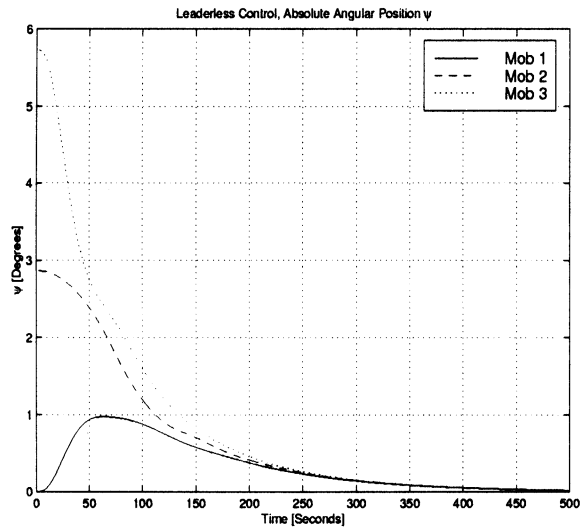

Figure 5. Absolute Angular Position ψ, Leaderless Control

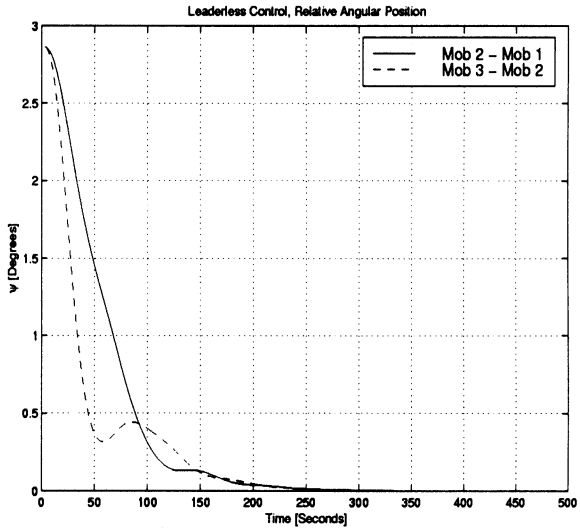

Figure 6. Relative Angular Position, Leaderless Control

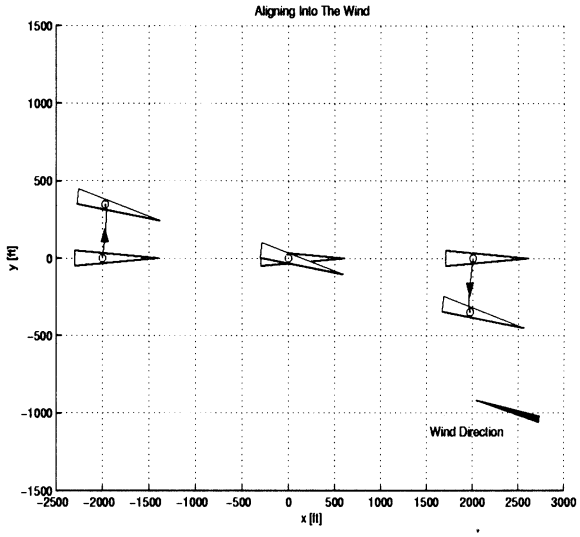

Figure 7. Aligning Into the Wind

This particular motion represents the rotation of the MOB into the wind. Figure 7 displays the motions of all three vessels during this maneuver (note: the triangles representing the vessels are not drawn to scale). Only the results with leaderless control are included here since the leaderless scheme outperforms the follow-the-leader scheme as illustrated previously. The second figure, Figure 8, contains plots of the relative angular positions of the vessels. Clearly the controller helps to bring the MOB into alignment as the relative errors between vessels decrease with time and eventually go to zero (perfect angular alignment).

IV. CONCLUSION

A fully nonlinear DP controller for a single MOB vessel was developed in both robust and parameter adaptation versions. The controller utilizes Multiple Sliding Surfaces (MSS), Dynamic Surface Control (DSC), and the Slotine and Li algorithm. This technique was then extended to the control of multiple vessels. Sliding surfaces for follow-the-leader and leaderless control approaches were formulated. The robust form of these multiple vessel control schemes were then simulated in Shift (as well as Matlab for verification) for an MOB consisting of three vessels.

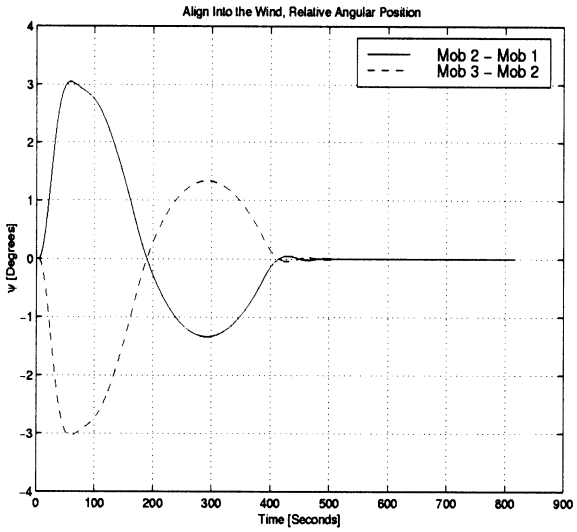

Figure 8. Relative Angular Position, Aligning Into the Wind

It was found that leaderless control is better able to keep the MOB aligned than the various follow-the-leader schemes presented. Leaderless control is also able to adequately rotate the MOB while maintaining tight alignment constraints.

Areas of current and future work will encompass the implementation of the adaptive algorithm for multiple vessels, optimal trajectory generation, and the simulation of higher level maneuvers.

REFERENCES

Fossen, TI (1994). *Guidance and Control of Ocean Vehicles*, Wiley, New York.

Newman, JN (1977). *Marine Hydrodynamics*, MIT Press, Cambridge, MA.

Slotine, JJE, and Li, W (1991). *Applied Nonlinear Control*, Prentice-Hall, Englwood Cliffs, NJ.

Shift (1996-1997). "Shift Release Notes and User Manuals", *http://www.path.berkeley.edu/shift/publications.html*, California PATH.

Swaroop, D, Hedrick, JK, Yip, PP, and Gerdes, JC (1997). "Dynamic Surface Control of Nonlinear Systems", *Proceedings of the 1997 American Control Conference*, Albuquerque, NM.

Swaroop, D, and Hedrick, JK (1996). "String Stability of Interconnected Systems", *IEEE Transactions on Automatic Control*, Vol. 41, no. 3, pp. 349–357.

Won, M, and Hedrick, JK (1996). "Multiple Surface Sliding Control of a Class of Uncertain Nonlinear Systems", *International Journal of Control*, Vol. 64, No. 4.